BMC Genomics

RESEARCH

Open Access

Characteristic analysis of N^6-methyladenine in different parts of yak epididymis

Ziqiang Ding[1,2], Xingdong Wang[1,2], Shaoke Guo[1,2], Yandong Kang[1,2], Mengli Cao[1,2], Liyan Hu[1,2], Ben Zhang[1,2], Lin Xiong[1,2], Jie Pei[1,2], Tao Yang[3*] and Xian Guo[1,2*]

Abstract

Background The epididymis is essential for sperm maturation. During sperm maturation, markable alterations of the payload of small noncoding RNAs are observed in the epididymis, which indicated the role of epigenetic alterations in sperm maturation. However, the N^6-Methyladenosine (m^6A) modification profile of the epididymis remains unelucidated. Therefore, in this study, we assessed the m^6A modification levels in the caput, corpus, and cauda of the yak epididymis using a combination of methylated RNA immunoprecipitation and RNA sequencing.

Results The m^6A levels were significantly increased in the corpus of the epididymis. Functional enrichment analysis of differentially methylated RNA (DMR) between the corpus and caput group revealed the significant enrichment of DMRs in the gap junction, ErbB signaling pathway, and mTOR signaling pathway, which participate in cell communication and sperm maturation. In addition, the DMRs of cauda-vs-corpus group were enriched in apoptosis, the FoxO signaling pathway, the PI3K-Akt signaling pathway, and the tumor necrosis factor signaling pathway that were associated with sperm autophagy, oxidative stress, and sperm maturation. Furthermore, we identified the key genes exhibiting significant changes in m^6A levels but with no differences in RNA levels, including YY1-associated factor 2, forkhead box J2, and forkhead box O1. This finding indicated that m^6A modifications affect these genes during translation, thereby participating in sperm maturation.

Conclusions In summary, we generated the m^6A profile of the yak epididymis, which will aid in further elucidating the maturation process of sperm and reveal more information related to male infertility.

Keywords Epididymis, Reproductive physiology, N^6-Methyladenosine, Sperm maturation, Yak

Introduction

RNA modification regulates RNA to perform life activities. Among the identified RNA modifications, methylation accounts for approximately 60% of modifications, including 5-methylcytosine, N^6-methyladenosine (m^6A), and N^6–2'-O-methyladenosine [1, 2]. In mammals, m^6A is one of the most common RNA modifications that participates in the post-transcriptional regulation of different RNA types; and it can affect RNA stability, translation, and higher structure to regulate physiological and pathological processes, including cell development, gametogenesis, hematopoiesis, and tumor generation [3–6]. Studies on m^6A in different species and tissues have revealed that RRACH (R=G/A, H=A/U/C) is the

*Correspondence:
Tao Yang
ding20241230@163.com
Xian Guo
guoxian@caas.cn
[1] Key Laboratory of Yak Breeding of Gansu Province, Lanzhou Institute of Husbandry and Pharmaceutical Sciences, Chinese Academy of Agricultural Sciences, Lanzhou 730050, China
[2] Key Laboratory of Animal Genetics and Breeding on Tibetan Plateau, Ministry of Agriculture and Rural Affairs, Lanzhou 730050, China
[3] Haibei Animal Husbandry Science and Technology Demonstration Park Management Committee, Haibei 810299, China

conserved sequence of the most common m^{6}A modification site, and the sequence is primarily located near stop codons and 3′-untranslated regions (3′-UTRs) [7–9]. In addition, m^{6}A modification is a dynamically reversible process under the various proteins participating, such as methyltransferases (methyltransferase 3 (METTL3), methyltransferase 14 (METTL14), Wilms' tumor 1-associating protein (WTAP), and vir-like m6 A methyltransferase associated (VIRMA)), demethylases (fat mass and obesity-associated protein (FTO) and AlkB homolog 5 (ALKBH5)), and m^{6}A-binding proteins (YTH family proteins). Therefore, it can shape the fate of RNA in an m^{6}A methylation-dependent manner [9–14]. Furthermore, this fate is a significant factor that affects spermatogenesis and maturation.

Spermatogenesis and maturation encompass continuous and complex biological processes. Haploid round sperm cells are generated after mitosis and meiosis. Thereafter, molecular rearrangements and biochemical changes occur to generate the mature sperm [15, 16]. The proteins associated with m^{6}A modification undergo dynamic alteration during different spermatogenesis stages of mice,, with differences in their overall distribution [17]. The single-cell sequencing study revealed that RNA m^{6}A regulatory factors are expressed in almost all testicular cell types, including somatic and germ cells [18]. In mouse, the volume and weight of testis were significantly decreased, spermatocyte differentiation was abnormal, and spermatogenesis was interrupted after knocking out YTH domain containing 2 (YTHDC2), a m^{6}A reader protein, and resulting in infertility [13]. Similarly, *YTHDC2* missense and mutation heterozygotes exhibited the same reproductive defects [19, 20]. In addition, the m^{6}A modification related proteins, such asMETTL3 and METTL14 also participate in spermatogenesis by regulating the differentiation of spermatogonial cells and the initiation of meiosis [15, 21]. In mouse, m^{6}A levels were significantly decreased in sperm cells, meiosis-associated genes were significantly downregulated, and sperm quantity and vitality were significantly decreased after knocked out METTL3 and/or METTL14, and the phenotype is similar to human oligoasthenoteratozoospermia [17, 22]. ALKBH5 is a common m^{6}A eraser and highly expressed in the testes of male mice. ALKBH5 knockout increased m^{6}A modification levels of mRNAs that involved in the P53 functional network, further resulted in 3′-UTR splicing disorder, thereby inhibiting meiosis and testicular atrophy [23, 24]. Single-cell sequencing of the human non-obstructive azoospermia testes revealed the dysregulation of almost all RNA m^{6}A regulatory factors [25, 26]. Collectively, these findings verify the essential role of m^{6}A modification and its associated genes in spermatogenesis.

The epididymis is a tubular tissue connected to the testis. It can continuously modify the sperm, alter sperm membrane components, and allow the sperm to acquire motility and fertilization abilities [27]. However, insufficient sperm maturation in the epididymis or the disorders of epigenetic modifications can severely affect sperm quality, resulting in azoospermia, teratozoospermia, or asthenozoospermia, which ultimately results in male infertility [18, 28–30]. Notably, the epigenetic characteristics of the sperm are remodeled in the epididymis, with changes in their chromatin configuration that was associated with DNA methylation [31]. Both environmental stress and DNA released by epididymal somatic cells, particularly the transient DNA methylation process, affect the DNA methylation of the sperm [12, 32, 33]. Moreover, the RNA payload occurred significant changes as the sperm travels along the epididymis,, including modifications in microRNA, ribosomal RNA content, and the 20-nt long piRNA, which may be associated with sperm epigenetics [34–37]. Unfortunately, the RNA methylation profile of the epididymis remains uninvestigated. This investigation may facilitate the correct maturation and fertilization of sperm, revealing more information on male infertility.

Therefore, in this study, we determined the m^{6}A levels in the caput, corpus, and cauda of the epididymis of adult yaks using methylated RNA immunoprecipitation sequencing (MeRIP-seq) and RNA sequencing (RNA-seq) and constructed an m^{6}A map of the transcriptomes in the different epididymal regions. Our findings may provide novel insights into the modifications needed for sperm maturation in the epididymis.

Results

Observation of tissue structure and m6 A levels in different epididymal regions

The epididymis is an essential organ for sperm modification and maturation. Morphological comparisons among different regions of the epididymis (Fig. 1A) revealed the presence of densely packed and larger-diameter tubules in the epididymal caput. Furthermore, thicker tubule walls and a higher number of epithelial cells were present in the epididymal corpus. Sperm count was higher in the epididymal cauda, playing a role in storage. Next, we determined whether differences exist in the m^{6}A levels in among different regions of epididymal. We observed significant differences in m^{6}A levels in the epididymal caput, corpus, and cauda ($P < 0.05$); the highest m^{6}A levels were noted in the epididymal corpus (Fig. 1B). Furthermore, significant differences were noted in the genes associated with m^{6}A readers, writers, and erasers in the different epididymal regions (Fig. 1C and D). Among the three epididymal regions, the expression of the m^{6}A

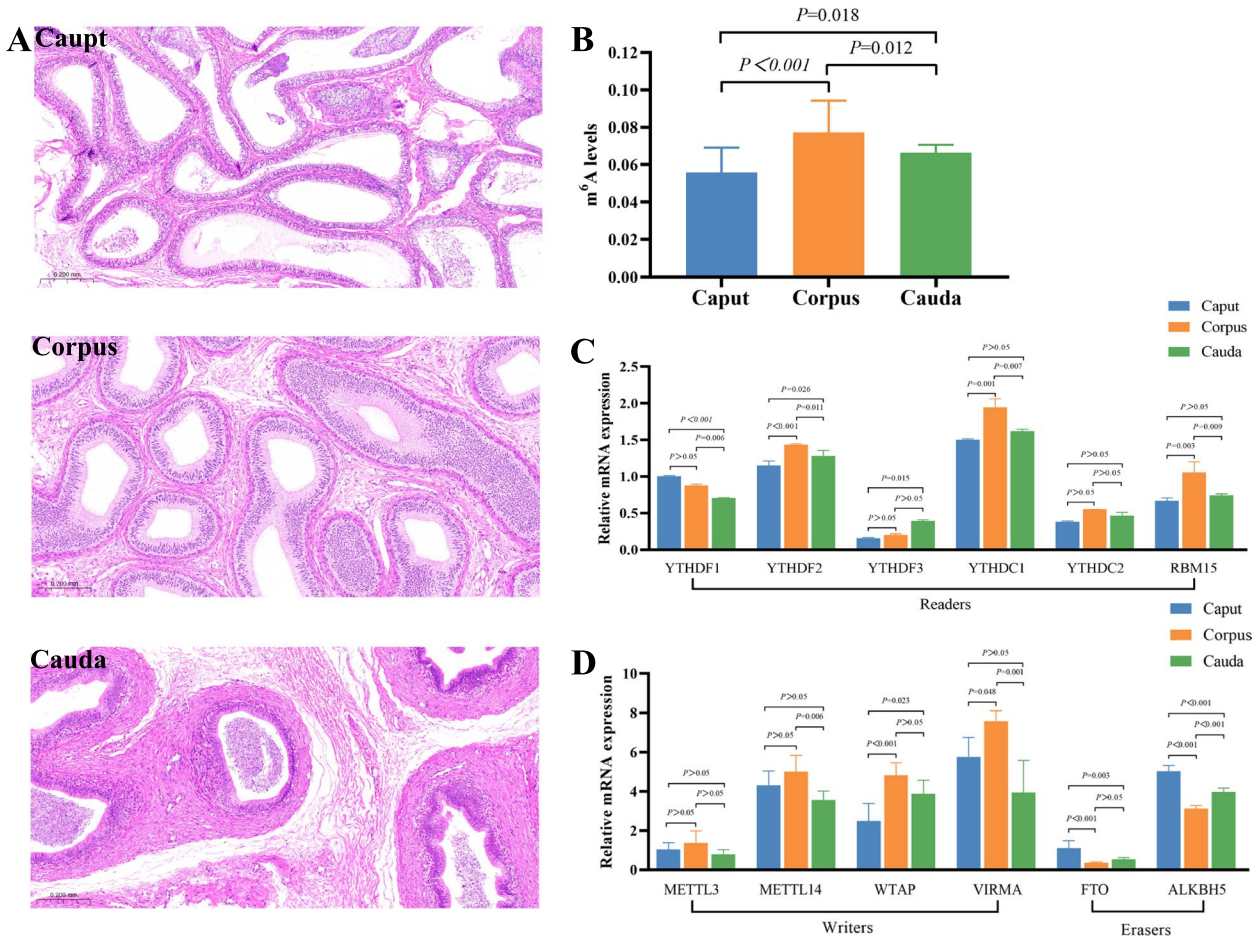

Fig. 1 Histological observation of the epididymal regions and measurement of m^{6}A levels. **A** Histological observation of the epididymal caput, corpus, and cauda (15×). **B** m^{6}A levels in the different epididymal regions. **C** Expression of m^{6}A reader-related genes in among different regions of epididymal. **D** Expression of m^{6}A writer and eraser-related genes in among different regions of epididymal

readers and writer-related genes (*YTHDF2, YTHDC1, RBM15, METTL14, WTAP, VIRMA*) was the highest in the epididymal corpus; however, the expression of the m^{6}A eraser-related genes *FTO* and *ALKBH5* was significantly downregulated ($P < 0.05$). Collectively, these findings suggest differences in m^{6}A levels among different epididymal regions. Therefore, different physiological functions may occur during sperm maturation.

MeRIP-seq results and analysis of among different regions of epididymal

We subjected the epididymal caput, corpus, and cauda to MeRIP-seq analysis to elucidate the differences in m^{6}A modification across various epididymal regions. A higher number of m^{6}A peaks was observed in the epididymal caput and cauda (Fig. 2A). Methylation peak annotation using ChIPseeker software revealed exons and 3′-UTRs as the primary distribution regions of the methylation peaks (Fig. 2B and C), consistent with previous reports on yak enrichment results [38]. Specific motifs are more prone to m^{6}A modification, this may be associated with specific biological functions [7]. Motif analysis of the epididymal caput, corpus and cauda revealed the presence of the canonical m^{6}A motif "RRACH" (Fig. 2D). This result indicates the high credibility of the identified m^{6}A peaks. Genomic distribution analysis revealed the differential distribution of m^{6}A peaks across yak chromosomes, with a major distribution on chromosomes 3, 8, and 19 (Fig. 2E, Supplementary Table 2). The visualization of randomly selected RNAs (*SRD5 A1* and *SP1*) with m^{6}A modifications in the 3′- and 5′-UTRs confirmed the m^{6}A occurrence sites (Fig. 2F).

Analysis of differentially methylated peaks (DMPs) among different epididymal regions

DMPs were selected in the epididymal corpus-vs-caput and cauda-vs-corpus groups using the criteria $P < 0.05$ and $|\log_2\text{FoldChange}| > 0.58$) and subjected to

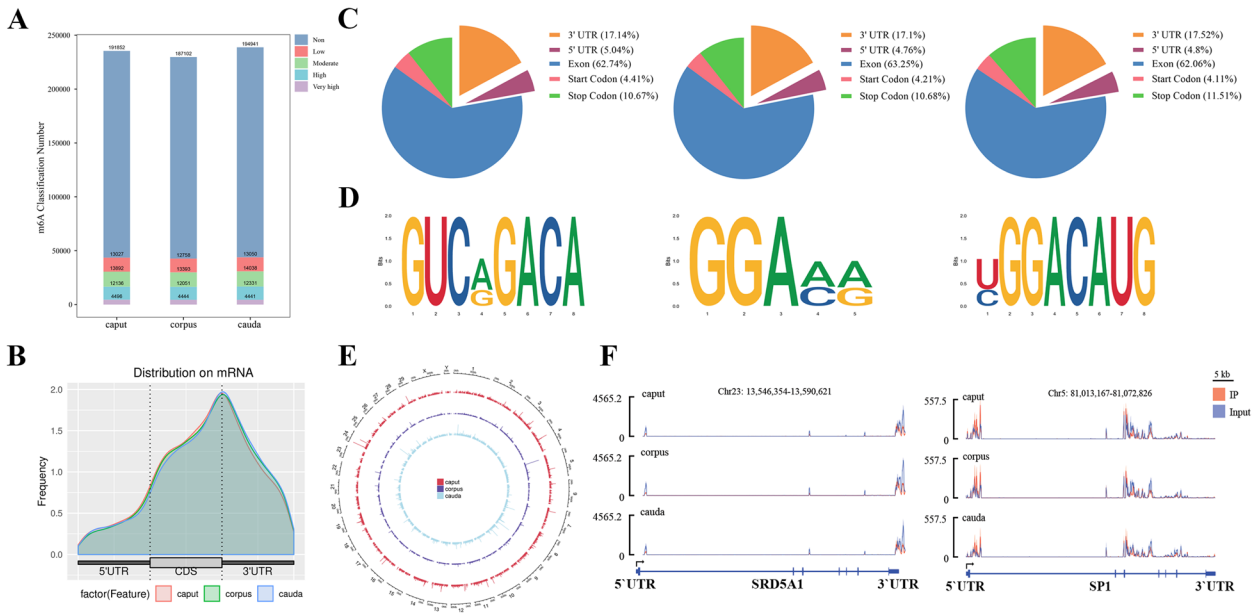

Fig. 2 Distribution characteristics and visualization analysis of m^{6}A in among different regions of epididymal. **A** Number of m^{6}A peaks with different methylation degrees in the epididymal caput, corpus, and cauda. **B** Statistics of the enrichment positions of the m^{6}A peak in among different regions of epididymal. **C** Peaks annotation and classification in the gene functional element regions. **D** m^{6}A peak enrichment of the top motif. **E** Site distribution map of the m^{6}A peaks compared with the yak reference genome. **F** Visual analysis of the m^{6}A peaks in *SRD5 A1* and *SP1*

enrichment analysis. A total of 790 DMPs were identified in the corpus-vs-caput group, including 308 hypermethylated peaks and 482 hypomethylated peaks. Furthermore, in the cauda-vs-corpus group, 435 hypermethylated and 284 hypomethylated peaks were identified (Fig. 3A, Supplementary Table 3). Figure 3B illustrated the overall distribution of these DMPs.

Nextly, to understand the potential effect of differential methylation, the differentially methylated RNAs (DMRs) in the two comparative groups were subjected to enrichment analysis. In KEGG enrichment analysis, the DMRs in both comparative groups were significantly enriched in the thyroid hormone signaling pathway, Wnt signaling pathway, and Hippo signaling pathway. Notably, the gap junction, ErbB signaling pathway, and mTOR signaling pathway were significantly enriched in the corpus-vs-caput group. In contrast, the differences were not significant in the cauda-vs-corpus group. This indicates that these signaling pathways play a key role in the epididymal caput and corpus during continuous sperm modifications in the epididymis. Similarly, in the cauda-vs-corpus group, DMRs were significantly enriched for apoptosis, the nuclear factor-kappa B signaling pathway, the Toll-like receptor signaling pathway, and the B cell receptor signaling pathway; these are classical pathways associated with cell apoptosis and immunity. Nevertheless, these pathways were not significant in the corpus-vs-caput group (Fig. 3C, Supplementary Table 4).

GO enrichment analysis revealed that the DMRs in the corpus-vs-caput group were enriched for the terms centrosome and nucleoplasm (ontology: cellular component), beta-catenin-TCF complex assembly and cytoplasmic microtubule organization (ontology: biological process), and ATP binding and microtubule binding (ontology: molecular function). On the other hand, the DMRs in the cauda-vs-corpus group were enriched for the terms cytosol and nucleoplasm (ontology: cellular component), lamellipodium assembly and negative regulation of neuron apoptotic process (ontology: biological process), and phosphotyrosine residue binding and thiol-dependent ubiquitin-specific protease activity (ontology: molecular function) (Fig. 3D, Supplementary Table 4).

Screening and identification of differentially expressed genes (DEGs)

RNA-seq data can serve as a background for MeRIP-seq data and facilitate basic RNA analysis. In this study, the overall gene expression was similar in the epididymis caput, corpus, and cauda. Figure 4A illustrated the FPKM values. Based on the criteria of $P < 0.01$ and $|\log_2\text{FoldChange}| > 1$, 2620 DEGs were identified in the corpus-vs-caput comparison group: 735 genes were upregulated and 1885 were downregulated. On the other hand, 1220 upregulated and 588 downregulated genes were identified in the cauda-vs-corpus comparison group (Fig. 4B, Supplementary Table 5). Figure 4C illustrated the

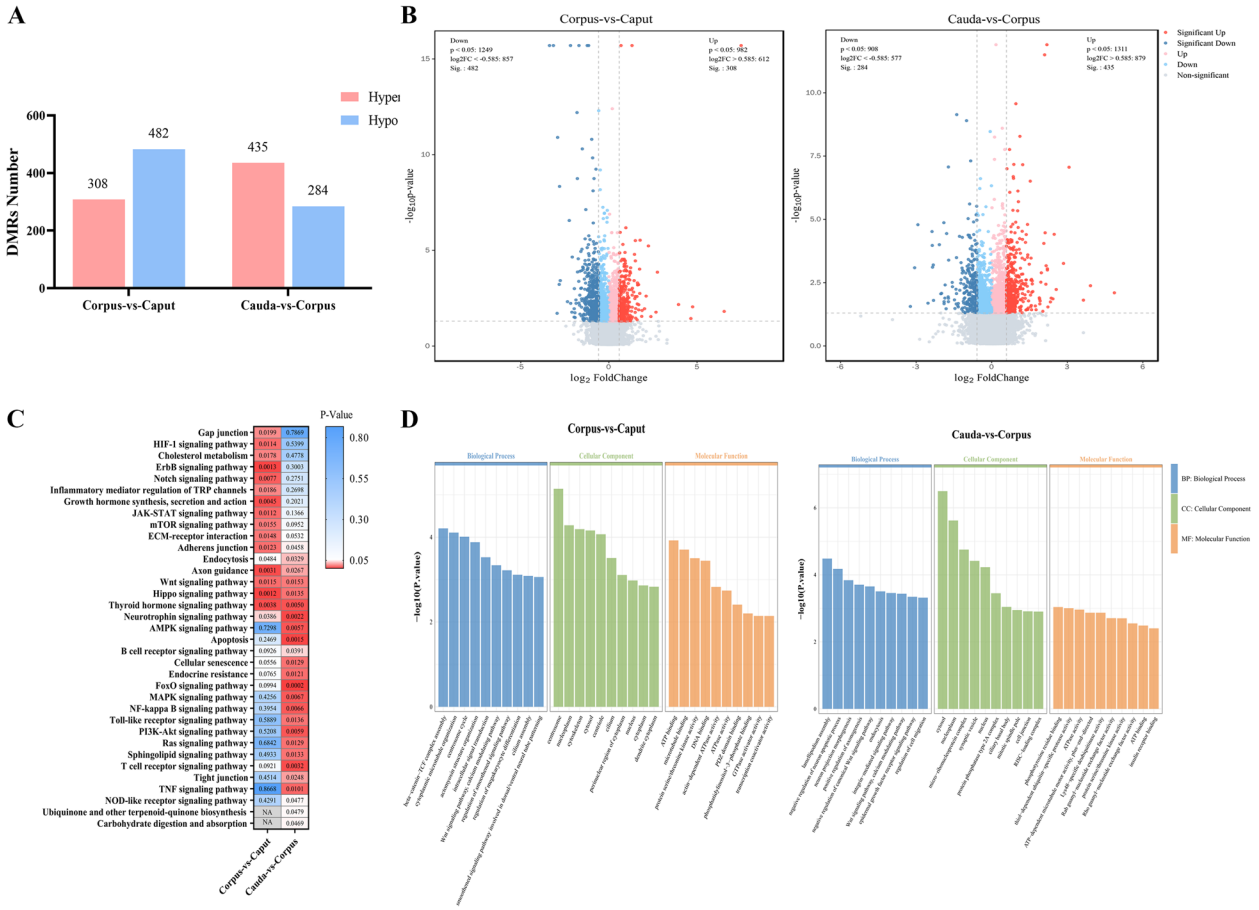

Fig. 3 Differentially methylated peak (DMP) and enrichment analyses of the yak epididymal caput, corpus, and cauda. **A** Number of DMPs in the corpus-vs-caput and cauda-vs-corpus comparison groups. **B** Volcano maps of the distribution of DMPs in the two comparison groups. **C** KEGG enrichment analysis of DMPs. **D** GO enrichment analysis. GO enrichment analysis showing the top 10 enrichment entries in each ontology

distribution pattern of the identified DEGs. GO enrichment analysis revealed the significant enrichment of the terms reproduction, motile cilium, and calcium ion binding in both comparison groups (Fig. 4D, Supplementary Table 6). Similarly, KEGG analysis of the corpus-vs-caput and cauda-vs-corpus groups revealed that the DEGs were significantly enriched for the AMPK and PPAR signaling pathways. Furthermore, in the corpus-vs-caput comparison groups, the DEGs were significantly enriched for arginine biosynthesis, steroid biosynthesis, and the cAMP signaling pathway. On the other hand, KEGG enrichment analysis of the cauda-vs-corpus comparison group revealed the significant enrichment of DEGs for pathways such as arachidonic acid metabolism, ferroptosis, and extracellular matrix–receptor interaction (Fig. 4E, Supplementary Table 6). GSEA analysis revealed the significant enrichment of mineral absorption in the epididymis corpus; while, xenobiotic metabolism by cytochrome P450 was significantly enriched in the epididymis cauda.

Combined analysis of m6 A-seq and RNA-seq data

The obtained m^{6}A-seq and RNA-seq data were combined and analyzed to explore the potential relationship between m^{6}A modification and genes. Based on the criteria of $P < 0.05$ and $|\log_2\text{FoldChange}| > 0.58$, 287 co-DEGs were identified in the corpus-vs-caput comparison group; among them, 89 genes exhibited m^{6}A hypermethylated peaks, 66 were upregulated, and 23 were downregulated. Among the 198 genes with m^{6}A hypomethylated peaks, 26 genes were upregulated, whereas 172 were downregulated. On the other hand, 188 co-DEGs were identified in the cauda-vs-corpus comparison group; among them, 122 genes exhibited m^{6}A hypermethylated peaks, with 101 being upregulated and 21 being downregulated. Furthermore, among the 66 genes with m^{6}A hypomethylated peaks, 16 were upregulated, whereas 50 were downregulated (Fig. 5A, Supplementary Table 7). In addition, genes with m^{6}A modifications ($P < 0.05$) but insignificant RNA expression were screened. This suggests that these m^{6}A occurrences affect RNA translation (Supplementary

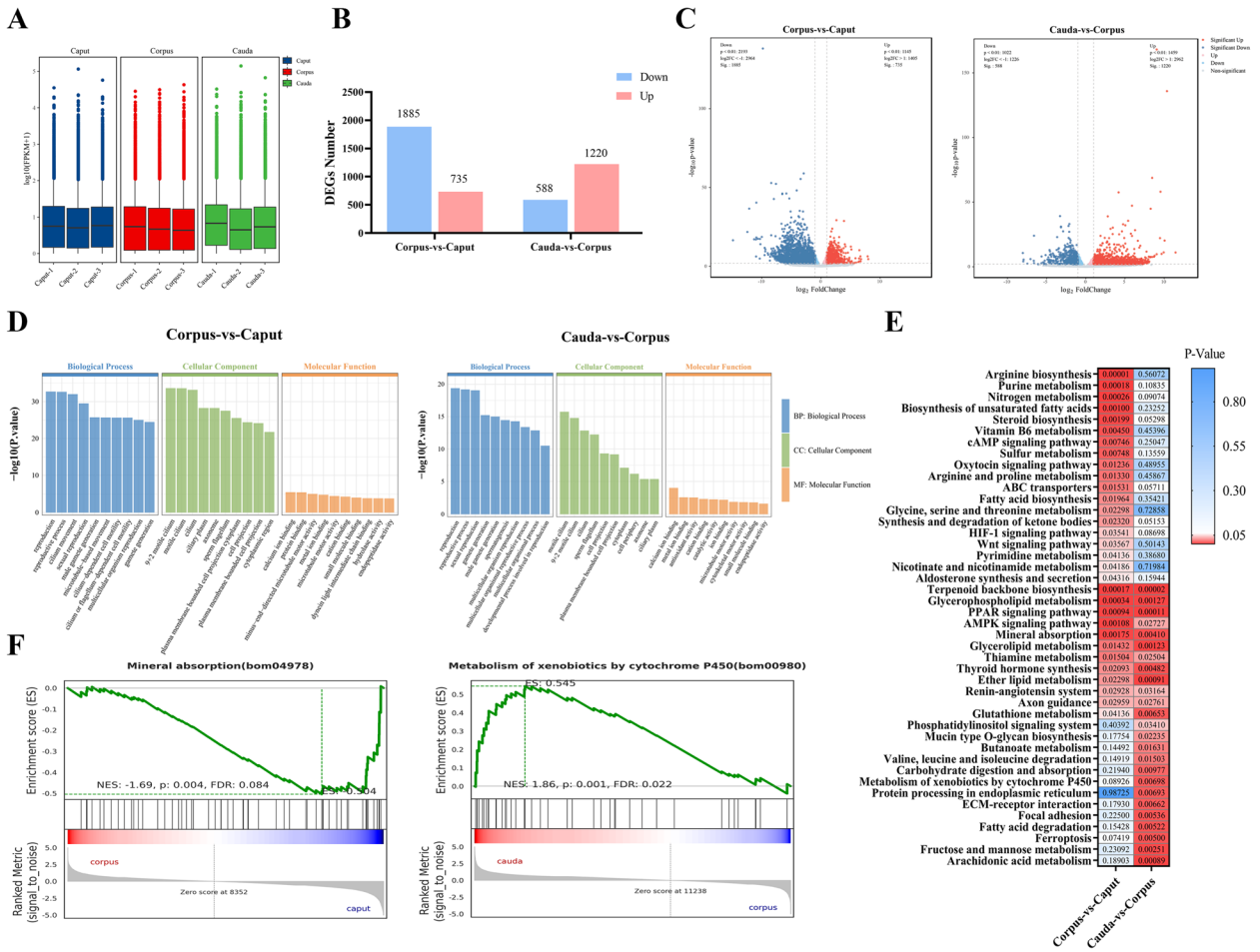

Fig. 4 Differentially expressed genes (DEGs) in the yak epididymal caput, corpus, and cauda. **A** Distribution map of the FPKM values of the epididymal caput, corpus, and cauda genes. **B** Number of DEGs in the corpus-vs-caput and cauda-vs-corpus comparison groups. **C** Volcano map showing the distribution of DEGs. **D** GO enrichment analysis. **E** KEGG enrichment analysis. **F** GSEA of the screened pathways

Table 8). Randomly selected genes with significant differences in RNA-seq data were subjected to qRT-PCR validation. The comparison revealed that the trends observed in qRT-PCR were consistent with the RNA-seq results (Fig. 5B).

Discussion

Yaks are important economic animals found throughout the Qinghai–Tibet Plateau, with a reputation for being versatile livestock [39]. However, increasing the number of yaks, decreasing the degeneration of offspring traits, and cultivating excellent breeds are challenges that should be urgently resolved [40]. m^{6}A modification plays a vital role in sperm production [18]. As a result, existing research primarily focuses on the potential regulatory role of m^{6}A during testis development and sperm production [38, 41]. Nevertheless, sperm does not have the ability to combine with eggs after being produced in the testis; it still needs to complete the "maturation" process in the epididymis. In this study, we generated a comprehensive m^{6}A methylation map of the epididymal caput, corpus, and cauda of male yaks and identified the potential m^{6}A regulatory genes associated with sperm maturation.

In this study, we observed significant differences in methylation levels in different epididymal regions. The m^{6}A levels were significantly higher in the epididymis corpus than in the epididymal caput and cauda. Subsequent analysis of m^{6}A-related regulatory genes revealed the significant upregulation of m^{6}A reader and writer-related genes in the epididymal corpus but the significant downregulation of the m^{6}A eraser genes FTO and ALKBH5. This may result in the accumulation of m^{6}A in the epididymal corpus. Another possible explanation is that during sperm movement from the epididymal caput to the cauda, the effective load of small noncoding RNA, particularly rsRNA and piRNA, significantly changes. These high-quality carriers of epigenetic information are

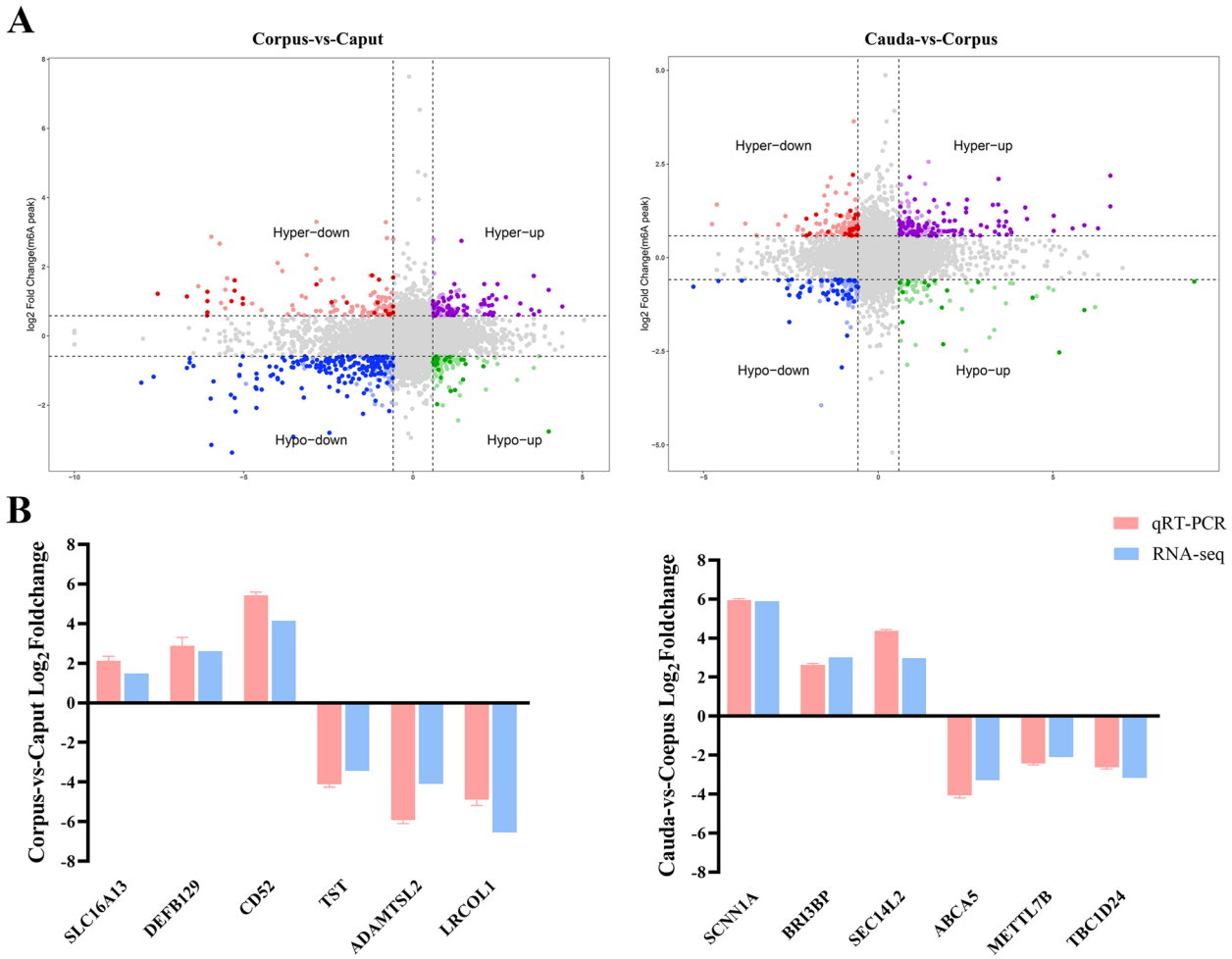

Fig. 5 Combined analysis and differential expression verification of m^{6}A-seq and RNA-seq data. **A** Nine-quadrant distribution plot showing the combined analysis of m^{6}A and RNA data. The bright-colored dots indicate genes with significant differences in both m^{6}A and RNA, whereas gray dots indicate the genes with no significant differences. **B** Validation of the differentially expressed genes identified via RNA-seq

exchanged in the epididymal corpus, increasing m^{6}A levels [34, 36, 37]. In addition, lower m^{6}A levels in the cauda epididymides may be beneficial for maintaining sperm motility (including forward and non-forward movements) and energy metabolism [42].

We also observed dynamic alterations in m^{6}A levels in different epididymal regions. This suggests that m^{6}A plays different physiological roles during sperm maturation. DMRs enrichment analysis revealed the significant enrichment of the gap junction, ErbB signaling pathway, and mTOR signaling pathway in the corpus-vs-caput comparison group; however, no differences were observed in the cauda-vs-corpus comparison group. Gap junctions are an important component of the epididymal barrier. They not only provide a mature environment for the sperm but also protect them from immune phagocytosis [43]. Furthermore, they participate in direct cell–cell communication and can rapidly respond to chemical stimuli; this is conducive to the rapid absorption of testicular fluid and release of substances required by sperm [43, 44]. The gap junction is also regulated by androgen signaling, which affects the process of Sertoli cell differentiation and sperm maturation [45]. Gap junctions can also promote the maturation of sperm tail structure and movement-related proteins, such as flagellin assembly, by regulating calcium signaling (such as the RHOA pathway) [46]. The ErbB signaling pathway can regulate the downstream MEK/MERK1/2 signaling pathway, which is involved in cell proliferation and differentiation. Furthermore, it can bind with androgens via nonreceptor pathways, particularly in the proximal epididymis, thereby promoting the biological function of androgens [47]. The enrichment of ErbB signaling pathway in the epididymis may also be related to the maintenance of a specific microenvironment [48]. ErbB signalingErbB1 can also affect sperm acrosome and flagellar structure and change

sperm motility by regulating fibroblast growth factor receptor [49]. Interestingly, the ErbB signaling pathway can directly or indirectly affect epididymal gap junctions and participate in sperm maturation [44, 47]. Moreover, the mTOR signaling pathway is significantly enriched in the corpus-vs-caput group. As a classical signaling pathway, mTOR participates in the differentiation of spermatogonial cells and regulates metabolism in supporting cells [50]. Recently, study have revealed that after the knockout of mTOR in the proximal epididymis, the differentiation potential of principal cells was impaired, the sperm transportation ability disappeared, and the sperm morphology was abnormal [51]. The mTOR signaling pathway may support sperm maturation and motility in the epididymis by regulating protein synthesis, energy metabolism, and cytoskeleton reorganization [52]. And the mTOR signaling pathway is also related to sperm epigenetic modification transmission and nutrient energy metabolism [53].

In the cauda-vs-corpus comparison group, the pathways associated with cell apoptosis, autophagy, immune regulation, and oxidative stress, including apoptosis, the FoxO signaling pathway, the PI3 K/Akt signaling pathway, and the TNF signaling pathway were significantly enriched [54–56]. Sperm is stored in the cauda epididymides and awaits fertilization, but prolonged retention can lead to oxidative stress and DNA damage. Therefore, the enrichment of these pathways is related to the identification and removal of abnormal sperm and the maintenance of storage environment [40]. In addition, the enrichment of autophagy function is also conducive to the removal of damaged organelles and the maintenance of cell status in epididymal cauda epithelial cells, thereby ensuring sperm quality [57]. Furthermore, we observed the significant enrichment of carbohydrate digestion and absorption in the cauda-vs-corpus group but not in the corpus-vs-caput group. This may be associated with the various uses of carbon sources in the epididymal cauda, including nourishing the sperm, granting them mobility before ejaculation, and maintaining the storage environment [58, 59]. Notable, DEG enrichment analysis of the RNA-seq data of this study revealed the significant enrichment of carbohydrate digestion and absorption in the cauda-vs-corpus group but not in the corpus-vs-caput group; this is similar to the DMRs enrichment results. However, additional studies are warranted to elucidate the potential physiological roles and functions of these DEGs.

The m^6A can affect RNA stability, translation, and higher structure of RNA [3]. In the present study, we focused on those genes with alterations at the m^6A level but with no differences at the RNA level; this may be associated with the regulation of RNA translation by m^6A. These include YY1-associated factor 2 (YAF2), forkhead box J2 (FOXJ2), and forkhead box O1 (FOXO1). We found that in both comparison groups, YAF2 exhibited a high methylation degree in both the epididymal caput and cauda. YAF2, a paralog of Yin-Yang 1 (YY1), can regulate the NF-kappa B and Wnt signaling pathways, which are involved in cell development, differentiation, and apoptosis, affecting ubiquitination modification and epigenetics [60–62]. Furthermore, YAF2 can rescue the phenotypic abnormalities caused by YY1-binding protein mutations, compensate for spermatocyte loss, and regulate meiosis and sperm movement [61, 63]. However, the methylation changes in YAF2 in all epididymal regions may be associated with regulating sperm maturation. Nevertheless, the specific regulatory mechanism should be explored.

FOXJ2 is a member of the forkhead box transcription factor family. It is specifically expressed in spermatocytes and round spermatid cells but not in elongating spermatids [64]. In a mouse FOXJ2 overexpression model, FOXJ2 increased testicular autophagy levels and inhibited meiosis, resulting in male infertility [65]. In addition, FOXJ2 can directly bind to connexin 43 (Cx43), upregulate Cx43 expression, and affect gap junctions, thereby resulting in male sterility [66]. In study on yak testicles, FOXJ2 has been noted to be highly methylated in sexually mature testicles, thereby participating in spermiogenesis [41].

In the present study, m^6A modification was observed in FOXO1; however, no changes were observed at the RNA level. At present, FOXO1 is known to play a vital role in cell apoptosis, oxidative stress, and glucose metabolism via phosphorylation and acetylation modifications [67]. Studies have revealed that FOXO1 inactivation will not prevent meiosis initiation; however, it will damage germ cells and result in defects in spermatogenesis, leading to the absence of mature sperm in the epididymal cauda. FOXO1 is a core factor in pig and mouse spermatogenesis [68, 69]. As a supplement, we observed the presence of m^6A modification in FOXO1 in the epididymal cauda, with high methylation; therefore, it may participate in sperm maturation.

Conclusion

In summary, we revealed the dynamic changes of methylation levels and m^6A modification between different epididymal regions. We observed significant differences in Gap junction, ErbB signaling pathway, mTOR signaling pathway, FoxO signaling pathway, PI3 K/Akt signaling pathway and TNF signaling pathway between different epididymal regions, which may affect sperm function maturation by synergistically regulating biological processes such as cell differentiation and apoptosis.

In addition, YAF2, FOXO1 and FOXJ2 may be important regulators of epididymal sperm maturation. Our results provide new insights into understanding the epigenetic molecular regulatory mechanisms of different epididymal regions and sperm maturation.

Materials and methods

Collection of epididymal samples

All animal-related procedures were performed according to the guidelines of the China Council on Animal Care and the Ministry of Agriculture of the People's Republic of China. The Animal Care and Use Committee of the Lanzhou Institute of Husbandry and Pharmaceutical Sciences Chinese Academy of Agricultural Sciences approved all yak-handling procedures (Permit No: LIHPS-2022-0144). Six 4-year-old healthy adult male yaks (*Bos grunniens,* 312.6 ± 17.3 kg) were selected from Gannan Tibetan Autonomous Prefecture (average altitude of 3000 meters), which were confirmed by veterinary examination to have no reproductive system diseases, free to eat local pasture and free to drink water. Use animal anesthetic with the trade name "Jingsongling", with a dosage of 0.05-0.2 mg/kg, for anesthesia. After anesthesia, iodine was used to locally disinfect the testicles, and then the veterinarian castrated all animals to collect epididymal tissue samples. Subsequently, the collected epididymal tissues were washed with physiological saline solution and dissected to separate the caput, corpus, and cauda regions based on anatomical landmarks. A part of the tissue was fixed with 4% neutral buffered formalin for histological analysis, whereas the remaining tissues were stored in liquid nitrogen for freezing until it was used for analysis.

Hematoxylin and eosin (H&E) staining

After fixation, epididymal tissue samples were dehydrated using 75% ethanol, embedded with paraffin, and sliced into 5-mm thick sections. The sections were stained using an improved H&E staining kit (SolarBio, Beijing, China) according to the manufacturer's instructions. Thereafter, the sections were sealed using neutral gum and imaged under the Pannoramic 250 digital section scanner (Drnjier, Jinan, China).

Measurement of m^6A levels

Total RNA was extracted by treating different regions of the isolated epididymis with TRIzol. A micro-nucleic acid analyzer was used to measure the absorbance A260/A280 value. Electrophoresis was performed to measure RNA purity and integrity. m^6A levels were measured in the different epididymal regions using a m^6A RNA methylation quantitative detection kit (Epigentek, NY, United States) according to the manufacturer's instructions. Each sample was analyzed three times. The absorbance was measured at 450 nm. The absorbance of the blank hole was subtracted during the calculation, and the final m^6A level was expressed as a percentage value.

cDNA synthesis and quantitative real-time polymerase chain reaction (qRT-PCR)

The Transcriptor First Strand cDNA Synthesis Kit (Transgen, Beijing, China) was used to reverse transcribe each RNA sample (diluted to 500 ng/mL). The cDNA was then stored at −80℃. Primers were selected based on the RNA-seq results. The selected genes were subjected to qRT-PCR analysis using the LightCycler® 96 Real-Time Detection System (Roche, Beijing, China). The internal reference gene was glyceraldehyde-3-phosphate dehydrogenase. The 20 μL reaction mixture comprised the following components: 10 μL of 2× SYBR Green II PCR Mix (Takara Bio), 1 μL cDNA (25 ng), 1 μL primers, and 8 μL nuclease-free water. The reaction conditions were as follows: 95℃ for 5 min, followed by 40 cycles at 95℃ for 10 s, 60℃ for 30 s, and 72℃ for 2 min. A melting curve was obtained from 65℃ to 95℃, which was increased in increments of 0.5℃ every 5 s. Relative expression was calculated using the $2^{-\Delta\Delta Ct}$ method. The primer sequences were listed in the Supplementary Table 1.

Library sequencing and bioinformatics analysis

The methods reported by Guo et al. [41]. were utilized to perform RNA extraction and quality control, library construction, sequencing, and bioinformatics analysis. Qualified RNA was reverse transcribed into cDNA. Oligo-dT magnetic beads were utilized to perform two purification rounds. For library construction and sequencing, mRNA was specifically captured using polyadenylate. Low-quality and N-base or low-quality reads were filtered and high-quality clean reads were retained. The clean reads were compared with the yak reference genome (LU_Bosgru_v3.0). Then, MeTDiff (v1.0, https://github.com/compgenomics/MeTDiff) [70] and ChIPseeker (v1.30.3, https://bioconductor.org/packages/release/bioc/html/ChIPseeker.html) [71] software were used to detect, annotate, and analyze the peak values of the samples using the following criteria: $P < 0.05$ and $|\log_2 FoldChange| > 0.58$. In the transcriptome sequencing data, HTSeq-count4 (v2.0.2, https://htseq.readthedocs.io/) was used to calculate the fragments per kilobase per million mapped fragment 3 of each gene and obtain the read counts of each gene. R (v3.2.0) was utilized to perform principal component analysis to evaluate the biological duplication of samples. The criterion for screening significantly enriched items in Gene Ontology (GO) and Kyoto Encyclopedia of Genes and Genomes (KEGG)

analyses was $P < 0.05$. Supplementary Document 1 summarizes the specific data analysis process.

Differential gene expression verification and statistical analysis

Based on the gene expression results, differential genes were randomly selected for verification. Supplementary Table 1 lists the primer sequences. The data were integrated and analyzed using SPSS 22.0. The results are expressed as mean ± standard error of the mean. One-way analysis of variance was used to perform data comparisons. $P < 0.05$ was selected as the significance threshold.

Abbreviations

m^{6}A	N^6-Methyladenosine
mTOR	Mammalian target of rapamycin
METTL3	Methyltransferase 3
METTL14	Methyltransferase 14
WTAP	Wilms' tumor 1-associating protein
VIRMA	Vir-like m6A methyltransferase associated
FTO	Fat mass and obesity-associated protein
ALKBH5	AlkB homolog 5
YTHDC2	YTH domain containing 2
SRD5 A1	Steroid 5 alpha-reductase 1
SP1	Sp1 transcription factor

Supplementary Information

The online version contains supplementary material available at https://doi.org/10.1186/s12864-025-11684-w.

Supplementary Material 1.

Authors' contributions

X.G. and Z.D. conceptualized this study. X.W. and S.G. helped in the investigation. Y.K., M.C., and L.H. helped in methodology and software. Z.D., B.Z., and L.X. performed data curation. Z.D. and J.P. helped in writing the original draft. X.G., T.Y., and Z.D. helped in writing, reviewing, and editing the manuscript. X.G. helped in funding acquisition. All authors contributed to the interpretation of the results and writing of the manuscript.

Funding

This study was financially supported by the National Key Research and Development Program of China (2022YFD1302103), China Agriculture Research System of MOF and MARA (CARS-37), and Innovation Project of Chinese Academy of Agricultural Sciences (25-LZIHPS-01).

Data availability

No datasets were generated or analysed during the current study.

Declarations

Ethics approval and consent to participate

The study was conducted according to the Declaration of Helsinki guidelines and was approved by the Institutional Animal Care and Use Committee of the Lanzhou Institute of Husbandry and Pharmaceutical Sciences of the Chinese Academy of Agricultural Sciences (LIHPS-2022-0144).

Consent for publication

Not applicable.

Competing interests

The authors declare no competing interests.

Received: 11 June 2024 Accepted: 7 May 2025
Published online: 19 May 2025

References

1. Scheitl CPM, GhaemMaghami M, Lenz A-K, Höbartner C. Site-specific RNA methylation by a methyltransferase ribozyme. Nature. 2020;587:663–7.
2. Xie S, Chen W, Chen K, Chang Y, Yang F, Lin A, et al. Emerging roles of RNA methylation in gastrointestinal cancers. Cancer Cell Int. 2020;20:585.
3. Wang X, Zhao BS, Roundtree IA, Lu Z, Han D, Ma H, et al. N(6)-methyladenosine modulates messenger RNA translation efficiency. Cell. 2015;161:1388–99.
4. Liu N, Pan T. N6-methyladenosine–encoded epitranscriptomics. Nat Struct Mol Biol. 2016;23:98–102.
5. Yang Y, Hsu PJ, Chen Y-S, Yang Y-G. Dynamic transcriptomic m6A decoration: writers, erasers, readers and functions in RNA metabolism. Cell Res. 2018;28:616–24.
6. Jiang X, Liu B, Nie Z, Duan L, Xiong Q, Jin Z, et al. The role of m6A modification in the biological functions and diseases. Signal Transduct Target Ther. 2021;6:74.
7. Dominissini D, Moshitch-Moshkovitz S, Schwartz S, Salmon-Divon M, Ungar L, Osenberg S, et al. Topology of the human and mouse m6A RNA methylomes revealed by m6A-seq. Nature. 2012;485:201–6.
8. Zhang H, Shi X, Huang T, Zhao X, Chen W, Gu N, et al. Dynamic landscape and evolution of m6A methylation in human. Nucleic Acids Res. 2020;48:6251–64.
9. Wang J, Wang J, Gu Q, Ma Y, Yang Y, Zhu J, et al. The biological function of m6A demethylase ALKBH5 and its role in human disease. Cancer Cell Int. 2020;20:347.
10. Wang X, Feng J, Xue Y, Guan Z, Zhang D, Liu Z, et al. Structural basis of N(6)-adenosine methylation by the METTL3-METTL14 complex. Nature. 2016;534:575–8.
11. Jia GX, Lin Z, Yan RG, Wang GW, Zhang XN, Li C, et al. WTAP function in sertoli cells is essential for sustaining the spermatogonial stem cell niche. Stem cell reports. 2020;15:968–82.
12. Galan C, Serra RW, Sun F, Rinaldi VD, Conine CC, Rando OJ. Stability of the cytosine methylome during post-testicular sperm maturation in mouse. PLoS Genet. 2021;17:e1009416.
13. Lasman L, Krupalnik V, Viukov S, Mor N, Aguilera-Castrejon A, Schneir D, et al. Context-dependent functional compensation between Ythdf m6A reader proteins. Genes Dev. 2020;34:1373–91.
14. Boulias K, Greer EL. Biological roles of adenine methylation in RNA. Nat Rev Genet. 2023;24:143–60.
15. Xu K, Yang Y, Feng G-H, Sun B-F, Chen J-Q, Li Y-F, et al. Mettl3-mediated m6A regulates spermatogonial differentiation and meiosis initiation. Cell Res. 2017;27:1100–14.
16. Cheuquemán C, Maldonado R. Non-coding RNAs and chromatin: key epigenetic factors from spermatogenesis to transgenerational inheritance. Biol Res. 2021;54:41.
17. Lin Z, Hsu PJ, Xing X, Fang J, Lu Z, Zou Q, et al. Mettl3-/Mettl14-mediated mRNA N6-methyladenosine modulates murine spermatogenesis. Cell Res. 2017;27:1216–30.
18. Cai Z, Niu Y, Li H. RNA N6-methyladenosine modification, spermatogenesis, and human male infertility. Mol Hum Reprod. 2021;27:gaab020.
19. Bailey AS, Batista PJ, Gold RS, Chen YG, de Rooij DG, Chang HY, et al. The conserved RNA helicase YTHDC2 regulates the transition from proliferation to differentiation in the germline. Elife. 2017;6:e26116.
20. Wojtas MN, Pandey RR, Mendel M, Homolka D, Sachidanandam R, Pillai RS. Regulation of m6A transcripts by the 3'→5' RNA Helicase YTHDC2 is essential for a successful meiotic program in the mammalian germline. Mol Cell. 2017;68:374-387.e12.
21. Gui Y, Yuan S. Epigenetic regulations in mammalian spermatogenesis: RNA-m6A modification and beyond. Cell Mol Life Sci. 2021;78:4893–905.
22. Zhang M, Nie J, Chen Y, Li X, Chen H. Connecting the dots: N6-Methyladenosine (m6 A) modification in spermatogenesis. Adv Biol (Weinh). 2023;7:e2300068.
23. Zheng G, Dahl JA, Niu Y, Fedorcsak P, Huang C-M, Li CJ, et al. ALKBH5 is a mammalian RNA demethylase that impacts RNA metabolism and mouse fertility. Mol Cell. 2013;49:18–29.

24. Tang C, Klukovich R, Peng H, Wang Z, Yu T, Zhang Y, et al. ALKBH5-dependent m6A demethylation controls splicing and stability of long 3'-UTR mRNAs in male germ cells. Proc Natl Acad Sci U S A. 2018;115:E325-33.
25. Wang M, Liu X, Chang G, Chen Y, An G, Yan L, et al. Single-cell RNA sequencing analysis reveals sequential cell fate transition during human spermatogenesis. Cell Stem Cell. 2018;23:599-614.e4.
26. Cai Z, Zhang J, Xiong J, Ma C, Yang B, Li H. New insights into the potential mechanisms of spermatogenic failure in patients with idiopathic azoospermia. Mol Hum Reprod. 2020;26:469–84.
27. Koch S, Acebron SP, Herbst J, Hatiboglu G, Niehrs C. Post-transcriptional Wnt signaling governs epididymal sperm maturation. Cell. 2015;163:1225–36.
28. van Tran N, Ernst FGM, Hawley BR, Zorbas C, Ulryck N, Hackert P, et al. The human 18S rRNA m6A methyltransferase METTL5 is stabilized by TRMT112. Nucleic Acids Res. 2019;47:7719–33.
29. Chen H, Alves MBR, Belleannée C. Contribution of epididymal epithelial cell functions to sperm epigenetic changes and the health of progeny. Hum Reprod Update. 2021;28:51–66.
30. Qin D, Gu Y, Zhang Y, Wang S, Jiang T, Wang Y, et al. Phase-separated CCER1 coordinates the histone-to-protamine transition and male fertility. Nat Commun. 2023;14:8209.
31. Capra E, Turri F, Lazzari B, Biffani S, Lange Consiglio A, Ajmone Marsan P, et al. CpG DNA methylation changes during epididymal sperm maturation in bulls. Epigenetics Chromatin. 2023;16:20.
32. Holland ML, Lowe R, Caton PW, Gemma C, Carbajosa G, Danson AF, et al. Early-life nutrition modulates the epigenetic state of specific rDNA genetic variants in mice. Science. 2016;353:495–8.
33. Chen H, Scott-Boyer M-P, Droit A, Robert C, Belleannée C. Sperm heterogeneity accounts for sperm DNA methylation variations observed in the caput epididymis, independently from DNMT/TET activities. Front Cell Dev Biol. 2022;10:834519.
34. Sellem E, Marthey S, Rau A, Jouneau L, Bonnet A, Le Danvic C, et al. Dynamics of cattle sperm sncRNAs during maturation, from testis to ejaculated sperm. Epigenetics Chromatin. 2021;14:24.
35. Sharma U, Conine CC, Shea JM, Boskovic A, Derr AG, Bing XY, et al. Biogenesis and function of tRNA fragments during sperm maturation and fertilization in mammals. Science. 2016;351:391–6.
36. Sharma U, Sun F, Conine CC, Reichholf B, Kukreja S, Herzog VA, et al. Small RNAs are trafficked from the epididymis to developing mammalian sperm. Dev Cell. 2018;46:481-494.e6.
37. Chen Q, Yan W, Duan E. Epigenetic inheritance of acquired traits through sperm RNAs and sperm RNA modifications. Nat Rev Genet. 2016;17:733–43.
38. Wang X, Pei J, Guo S, Cao M, Bao P, Xiong L, et al. Characterization of N6-methyladenosine in domesticated yak testes before and after sexual maturity. Front Cell Dev Biol. 2021;9:755670.
39. Tiwari M, Gujar G, Shashank CG, Ponsuksili S. Selection signatures for high altitude adaptation in livestock: a review. Gene. 2024;927:148757.
40. Ding Z, Xiong L, Wang X, Guo S, Cao M, Kang Y, et al. Comparative analysis of epididymis cauda of yak before and after sexual maturity. Animals (Basel). 2023;13:1355.
41. Guo S, Pei J, Wang X, Cao M, Xiong L, Kang Y, et al. Transcriptome studies reveal the N6-Methyladenosine differences in testis of yaks at Juvenile and sexual maturity stages. Animals (Basel). 2023;13:2815.
42. Yang Y, Huang W, Huang J-T, Shen F, Xiong J, Yuan E-F, et al. Increased N6-methyladenosine in human sperm RNA as a risk factor for asthenozoospermia. Sci Rep. 2016;6:24345.
43. Cyr DG, Dufresne J, Gregory M. Cellular junctions in the epididymis, a critical parameter for understanding male reproductive toxicology. Reprod Toxicol. 2018;81:207–19.
44. Kidder GM, Cyr DG. Roles of connexins in testis development and spermatogenesis. Semin Cell Dev Biol. 2016;50:22–30.
45. Zhang DC, Chen R, Cai YH, Wang JJ, Yin C, Zou K. Hyperactive reactive oxygen species impair function of porcine Sertoli cells via suppression of surface protein ITGB1 and connexin-43. Zool Res. 2020;41:203–7.
46. Skerrett-Byrne DA, Anderson AL, Bromfield EG, Bernstein IR, Mulhall JE, Schjenken JE, et al. Global profiling of the proteomic changes associated with the post-testicular maturation of mouse spermatozoa. Cell Rep. 2022;41:111655.
47. Dubé E, Dufresne J, Chan PTK, Cyr DG. Epidermal growth factor regulates connexin 43 in the human epididymis: role of gap junctions in azoospermia. Hum Reprod. 2012;27:2285–96.
48. Sipilä P, Björkgren I. Segment-specific regulation of epididymal gene expression. Reproduction. 2016;152:R91-99.
49. Saucedo L, Sobarzo C, Brukman NG, Guidobaldi HA, Lustig L, Giojalas LC, et al. Involvement of fibroblast growth factor 2 (FGF2) and its receptors in the regulation of mouse sperm physiology. Reproduction. 2018;156:163–72.
50. Deng CY, Lv M, Luo BH, Zhao SZ, Mo ZC, Xie YJ. The role of the PI3K/AKT/mTOR signalling pathway in male reproduction. Curr Mol Med. 2021;21:539–48.
51. Dou Z. The role of mTOR signaling pathway in the initial segment of mouse epididymis. JiNan. Shandong University. 2023. https://doi.org/10.27272/d.cnki.gshdu.2023.006365.
52. Lang X, Adjei M, Wang C, Chen X, Li C, Wang P, et al. RNA-Seq reveals the functional specificity of epididymal caput, corpus, and cauda genes of cattleyak. Anim Sci J. 2022;93:e13732.
53. Zhu Z, Yue Q, Xie J, Zhang S, He W, Bai S, et al. Rapamycin-mediated mTOR inhibition impairs silencing of sex chromosomes and the pachytene piRNA pathway in the mouse testis. Aging (Albany NY). 2019;11:185–208.
54. Kim S-J, Winter K, Nian C, Tsuneoka M, Koda Y, McIntosh CHS. Glucose-dependent insulinotropic polypeptide (GIP) stimulation of pancreatic beta-cell survival is dependent upon phosphatidylinositol 3-kinase (PI3K)/protein kinase B (PKB) signaling, inactivation of the forkhead transcription factor Foxo1, and down-regulation of bax expression. J Biol Chem. 2005;280:22297–307.
55. Xiao B, Li X, Feng XY, Gong S, Li ZB, Zhang J, et al. Restraint stress of male mice induces apoptosis in spermatozoa and spermatogenic cells: role of the FasL/Fas system†. Biol Reprod. 2019;101:235–47.
56. Juárez-Rojas L, Casillas F, López A, Betancourt M, Ommati MM, Retana-Márquez S. Physiological role of reactive oxygen species in testis and epididymal spermatozoa. Andrologia. 2022;54:e14367.
57. Yan Q, Wang Q, Nan J, Chen T, Wang J, Zhang Y, et al. Heme oxygenase 1 (HO1) regulates autophagy and apoptosis via the PI3K/AKT/mTOR signaling pathway of yak Sertoli cells. Theriogenology. 2024;220:96–107.
58. Tecle E, Gagneux P. Sugar-coated sperm: unraveling the functions of the mammalian sperm glycocalyx. Mol Reprod Dev. 2015;82:635–50.
59. Zhao W, Quansah E, Yuan M, Gou Q, Mengal K, Li P, et al. Region-specific gene expression in the epididymis of Yak. Theriogenology. 2019;139:132–46.
60. Liu Y, Hu G, Yang S, Yao M, Liu Z, Yan C, et al. Functional dissection of PRC1 subunits RYBP and YAF2 during neural differentiation of embryonic stem cells. Nat Commun. 2023;14:7164.
61. He Z, Yan RG, Zhang XN, Yang QE. Ring 1 and YY1 binding protein expressed in murine spermatocytes but dispensable for spermatogenesis. Genes (Basel). 2020;11:84.
62. Geng Z, Chen H, Zou G, Yuan L, Liu P, Li B, et al. Human amniotic fluid mesenchymal stem cell-derived exosomes inhibit apoptosis in ovarian granulosa cell via miR-369-3p/YAF2/PDCD5/p53 pathway. Oxid Med Cell Longev. 2022;2022:1–18.
63. Tian Q, Guo SM, Xie SM, Yin Y, Zhou LQ. Rybp orchestrates spermatogenesis via regulating meiosis and sperm motility in mice. Cell Cycle. 2020;19:1492–501.
64. Miao H, Miao CX, Li N, Han J. FOXJ2 controls meiosis during spermatogenesis in male mice. Mol Reprod Dev. 2016;83:684–91.
65. Bai FR, Wu QQ, Wu YJ, Hu YQ, Jiang ZX, Lv H, et al. Germline FOXJ2 overexpression causes male infertility via aberrant autophagy activation by LAMP2A upregulation. Cell Death Dis. 2022;13:665.
66. Bai FR, Wu QQ, Wu YJ, Fu L, Hu YQ, Jiang ZX, et al. [Impact of overexpressed FOXJ2 on mouse spermatogenesis and its action mechanism]. Zhonghua Nan Ke Xue. 2021;27:579–88.
67. Zhang M, Zhang Q, Hu Y, Xu L, Jiang Y, Zhang C, et al. miR-181a increases FoxO1 acetylation and promotes granulosa cell apoptosis via SIRT1 downregulation. Cell Death Dis. 2017;8:e3088.
68. Liu Z, Chen X, Zhang P, Li F, Zhang L, Li X, et al. Transcriptome-wide dynamics of m6A mRNA methylation during porcine spermatogenesis. Genomics Proteomics Bioinformatics. 2023;21:729–41.

69. Shen Z, Chen M, Gao Y, Dong F, Cen C, Wu H, et al. The function of Foxo1 in spermatogonia development is independent of PI3K/PTEN signaling. FASEB J. 2022;36:e22522.
70. Cui X, Zhang L, Meng J, Rao MK, Chen Y, Huang Y. MeTDiff: a novel differential RNA methylation analysis for MeRIP-Seq data. IEEE/ACM Trans Comput Biol Bioinform. 2018;15:526–34.
71. Yu G, Wang L-G, He Q-Y. ChIPseeker: an R/Bioconductor package for ChIP peak annotation, comparison and visualization. Bioinformatics. 2015;31:2382–3.

Publisher's Note